Differential thermopower of a CNT chiral carbon nanotube

Article *in* Journal of Physics Condensed Matter · May 2001

DOI: 10.1088/0953-8984/13/24/310

4 authors, including:

Samuel Yeboah Mensah
University of Cape Coast
83 PUBLICATIONS **318** CITATIONS

SEE PROFILE

N. G. Mensah
University of Cape Coast
51 PUBLICATIONS **209** CITATIONS

SEE PROFILE

G. Nkrumah
University of Ghana
8 PUBLICATIONS **66** CITATIONS

SEE PROFILE

Available at: http://www.ictp.trieste.it/~pub_off IC/2000/150

United Nations Educational Scientific and Cultural Organization
and
International Atomic Energy Agency
THE ABDUS SALAM INTERNATIONAL CENTRE FOR THEORETICAL PHYSICS

DIFFERENTIAL THERMOPOWER OF A CHIRAL CARBON NANOTUBE

S.Y. Mensah[1]
Department of Physics, Laser and Fibre Optics Centre, University of Cape Coast, Cape Coast, Ghana
and
The Abdus Salam International Centre for Theoretical Physics, Trieste, Italy,

F.K.A. Allotey
National Centre for Mathematical Sciences, Ghana Atomic Energy Commission, Kwabenya, Accra, Ghana
and
The Abdus Salam International Centre for Theoretical Physics, Trieste, Italy,

N.G. Mensah[1]
Department of Mathematics, University of Cape Coast, Cape Coast, Ghana

and

G. Nkrumah
Department of Physics, University of Ghana, Legon Accra, Ghana.

MIRAMARE – TRIESTE
October 2000

[1]Regular Associate of the Abdus Salam ICTP.

Abstract

Differential thermopower of a chiral carbon nanotube (CNT) was calculated using a tractable analytical approach. We obtained an expression for the electrical conductivity σ and the thermopower α. The results were numerically analysed. We noted from the values of α that the material can behave as a semimetal, n-type semiconductor and p-type as well, depending on the parameters of the CNT. We proposed the use of CNT as thermoelement.

1 Introduction

Research into the family of carbon based structures formed by wrapping graphite sheets into compact tube-shaped objects characterised by a chiral index (m,n), with m and n being two integers, which specify the carbon nanotube uniquely, has recently received a very big boost [1-3]. This is due to the fact that depending on the method of gluing, a set of atomic carbon structures with a wide spectrum of conducting properties is obtained. They range from insulating, semi-metallic or metallic behaviour to semiconductors with a gap of 0-2eV [4-7]. The unique conducting and capillary properties of the tubulenes make them promising materials for nanoelectronic devices.

Furthermore, there has been many suggestions to use the material as tips for scanning microscopy, ultrastrong mechanical fibre pinning sites for high T_c superconductors and inclusions in composites for body armour [8]. It is also noted that the carbon nanotube (CNT) is an ideal material to make field emitters because of its usually high aspect ratio as well as its mechanical and chemical stability. Many experiments with single-walled [9] and multi-walled [10-11] CNTs have demonstrated a relatively low threshold voltage of electron emission with little sample degradation [12].

The electronic properties of single-walled carbon nanotubes (SWNTs) have come under considerable attention currently. In [13] Kim *et al.* studied the electronic density of states (DOS) of SWNT and characterised sharp Van Hove singularities (VHS) in the DOS using scanning tunneling microscopy (STM) and compared their data to tight binding calculations for specific tube indices. In [14], a quantum-mechanical treatment of charge-carrier motion in the presence of an external magnetic field has been developed. Electron-photon interaction in CNTs has also been studied theoretically by Romanov [15], Kibis and Romanov [16], Chico *et al.* [17] and Langer *et al.* [18]. In [19], Woods and Mahan studied the electron-phonon effects in graphene and armchair (10,10) SWNT.

As stated in [20], two broad theoretical approaches for electron transport in nanotubes have emerged. The first approach comprises first principle numerical simulations as exemplified by Miyamoto *et al.* [21]. The other approach requires the creation of phenomenological models that yield somewhat rough but analytically tractable results [20]. The justification for the latter approach can be established from the work of Miyamoto *et al.* [21], where they computed the current excited in carbon and BC_2N nanotubes immersed in an electrostatic field. In that work they established that the current chiral angle (CCA) γ, which is equal to $\tan^{-1}(j_z/j_c)$ (where j_z is the current parallel to the tubular axis, i.e. z-axis, and j_c is the circumferential current), can be defined. Moreover, first principle calculation indicated that CCA is not equal to $\frac{\pi}{2}$ and is not equal to the geometric chiral angle (GCA) either, even though the surface conductivity of the monatomic curved surface of the CNT was taken to be isotropic. Kasumov *et al.* [22] and Langer *et al.*[18] measured the resistance of a SWNT, their data being in qualitative agreement

with theoretical results. Most importantly, the two experimental reports established the validity of theoretical models.

Thermoelectric properties have been studied in many materials over the past forty years with the understanding of determining a very good material for thermo devices. Unfortunately, these efforts have met with limited success owing to an accompanying degradation in electrical properties [23]. Relatively, recently, attention has been refocused, owing to the appearance of new materials like the multiquantum wells and superlattices [24]. Superlattices of semiconductors and semimetals are expensive for mass production, even though, they show enhancement in the thermoelectric figure of merit Z, hence the need to search for new materials.

In this paper, we study the differential thermopower of the chiral carbon nanotube. We use the approach in [24] together with the model developed in [20] to determine the thermopower α of the CNT. We observe that the thermopower strongly depends on GCA θ_h, electric field $\mathbf{E}$, temperature T, the real overlapping integrals for jumps along the tubular axis Δ_z and the base helix Δ_s. The manipulation of these parameters can give rise to high thermopower values, which in our opinion is highly recommendable.

This paper will be organised as follows: in section 2, we establish the theory and solution of the problem; in section 3, we discuss the results and draw conclusions.

2 Theory

We proceed as in [20] by considering an infinitely long chain of carbon atoms wrapped along a base helix as a model of a SWNT. The chief merit of this model is its analytical tractability, which readily yields physically interpretable results. Secondly, the model yields a correct qualitative description of various electronic processes which are corroborated by the first principle numerical simulations.

The problem is considered in the semiclassical approach by commencing with the Boltzmann kinetic equation [24],

$$\frac{\partial f(r,p,t)}{\partial t} + v(p)\frac{\partial f(r,p,t)}{\partial r} + eE\frac{\partial f(r,p,t)}{\partial p} = -\frac{f(r,p,t) - f_o(p)}{\tau}. \tag{1}$$

Here $f(r,p,t)$ is the distribution function; $f_o(p)$ is the equilibrium distribution function; $v(p)$ is the electron velocity; E is the applied electric field; r is the electron position, p is the electron dynamical momentum; τ is the electron relaxation time and e is the electron charge.

The collision integral is taken in the τ approximation and further assumed constant. The solution of Eq.(1) for a steady state is given by

$$\begin{aligned} f(p) &= \tau^{-1}\int_0^{\infty} \exp\left(-\frac{t}{\tau}\right) f_o(p - eEt)dt + \int_0^{\infty} \exp\left(-\frac{t}{\tau}\right) dt \\ &\cdot \left(\left[\varepsilon(p - eEt) - \mu\right] \frac{\nabla T}{T} + \nabla\mu \right) v(p - eEt) \frac{\partial f_o(p - eEt)}{\partial \varepsilon}, \end{aligned} \tag{2}$$

$\varepsilon(p)$ is the energy of the electron, and μ is the chemical potential. The current density is defined as

$$\boldsymbol{j} = e\sum_{p} \boldsymbol{v}(p) f(p). \tag{3}$$

Substituting Eq.(2) into Eq.(3) and making the transformation

$$p - eEt \rightarrow p,$$

we obtain for the current density

$$\begin{aligned} \boldsymbol{j} &= e\tau^{-1}\int_0^{\infty} \exp\left(-\frac{t}{\tau}\right) dt \sum_{p} \boldsymbol{v}(p - eEt) f_o(p) \\ &+e\int_0^{\infty} \exp\left(-\frac{t}{\tau}\right) dt \sum_{P} \left([\varepsilon(p) - \mu] \frac{\nabla T}{T} + \nabla\mu \right) \\ &\cdot \left(\boldsymbol{v}(p) \frac{\partial f_o(p)}{\partial \varepsilon} \right) \cdot \boldsymbol{v}(p - eEt) \end{aligned} \tag{4}$$

Now let's resolve the current along the tubular axis (z-axis) and the base helix respectively, neglecting the interference between the axial and the helical paths connecting a pair of atoms, so that transverse motion quantization is ignored. We then perform the following transformation

$$\sum_{p} \rightarrow \frac{2}{(2\pi\hbar)^2} \int\int dp_s dp_z,$$

and obtain the electron current density along the tubular axis and the base helix as

$$\begin{aligned} Z' &= \frac{2e^2\tau^{-1}}{(2\pi\hbar)^2} \int_0^{\infty} \exp\left(-\frac{t}{\tau}\right) dt \int\int v_z\left(p_z - eE_z t\right) f_o(p) dp_s dp_z \\ &+\frac{2e^2}{(2\pi\hbar)^2} \int_0^{\infty} \exp\left(-\frac{t}{\tau}\right) dt \int\int \left([\varepsilon(p) - \mu] \frac{\nabla_z T}{T} + \nabla_z \mu \right) \\ &\cdot \left(v_z\left(p_z\right) \frac{\partial f_o(p)}{\partial \varepsilon} \right) v_z\left(p_z - eE_z t\right) dp_s dp_z \end{aligned} \tag{5}$$

and

$$\begin{aligned} S' &= \frac{2e^2\tau^{-1}}{(2\pi\hbar)^2} \int_0^{\infty} \exp\left(-\frac{t}{\tau}\right) dt \int\int v_s\left(p_s - eE_s t\right) f_o(p) dp_s dp_z \\ &+\frac{2e^2}{(2\pi\hbar)^2} \int_0^{\infty} \exp\left(-\frac{t}{\tau}\right) dt \int\int \left([\varepsilon(p) - \mu] \frac{\nabla_s T}{T} + \nabla_s \mu \right) \\ &\cdot \left(v_s\left(p_s\right) \frac{\partial f_o(p)}{\partial \varepsilon} \right) v_s\left(p_s - eE_s t\right) dp_s dp_z \end{aligned} \tag{6}$$

where the integrations are carried out over the first Brillouin zone. From these two components, expressions for the axial and circumferential components of the current density emerge as follows:

$$j_z = Z' + S' \sin\theta_h, j_c = S' \cos\theta_h, \tag{7}$$

where, $\theta_\hbar$ is the GCA.

The energy of the electrons, as expressed in [20], is given as

$$\varepsilon(p) = \varepsilon_o - \Delta_z \cos\frac{p_z d_z}{\hbar} - \Delta_s \cos\frac{p_s d_s}{\hbar}, \tag{8}$$

where ε_o is the energy of an outer-shell electron in an isolated carbon atom, Δ_z and Δ_s are the real overlapping integrals for jumps along the respective co-ordinates, p_z and p_s are the carrier momentum along the tubular axis and the base helix respectively, $\hbar$ is the Planck's constant, d_z is the distance between the site n and the site $n+N$ along the tubular axis, and d_s is the distance between the site n and $n+1$ along the base helix.

To calculate the current density for non-degenerate electron gas, we use the Boltzmann equilibrium distribution function expressed as

$$f_o(p) = C\exp\left\{\frac{\Delta_z\cos\left(\frac{p_z d_z}{\hbar}\right) + \Delta_s\cos\left(\frac{p_s d_s}{\hbar}\right)}{kT}\right\}, \tag{9}$$

where

$$C = \frac{d_z d_s \mathrm{n}_o}{2I_0\left(\frac{\Delta_s}{kT}\right) I_0\left(\frac{\Delta_z}{kT}\right)},$$

n_o, is the surface charge density; $I_n(x)$ is the modified Bessel function of order n, and k is the Boltzmann's constant.

The components v_z and v_s of the electron velocity $\boldsymbol{v}$ are calculated from Eq.(8) as

$$v_z(p_z) = \frac{\partial\varepsilon}{\partial p_z} = \frac{\Delta_z d_z}{\hbar}\sin\left(\frac{p_z d_z}{\hbar}\right), \tag{10}$$

and

$$v_s(p_s) = \frac{\Delta_s d_s}{\hbar}\sin\left(\frac{p_s d_s}{\hbar}\right) \tag{11}$$

With the help of Eq.(5)-Eq.(11) and the fact that $E_s = E_z\sin\theta_h$ and $\nabla_s T = \nabla_z T\sin\theta_h$, we obtain for the axial j_z and circumferential j_c currents after cumbersome calculation, the following expression

$$\begin{aligned} j_z &= \left(\sigma_z(E) + \sigma_s(E)\sin^2\theta_h\right)\nabla_z\left(\frac{\mu}{e} - \phi\right) \\ &\quad - \left\{\sigma_z(E)\frac{k}{e}\left(\frac{\varepsilon_o-\mu}{kT} - \Delta_z^*\frac{I_0(\Delta_z^*)}{I_1(\Delta_z^*)} + 2 - \Delta_s^*\frac{I_1(\Delta_s^*)}{I_0(\Delta_s^*)}\right)\right. \\ &\quad \left. + \sigma_s(E)\frac{k}{e}\sin^2\theta_h\left(\frac{\varepsilon_o-\mu}{kT} - \Delta_s^*\frac{I_0(\Delta_s^*)}{I_1(\Delta_s^*)} + 2 - \Delta_z^*\frac{I_1(\Delta_z^*)}{I_0(\Delta_z^*)}\right)\right\}\nabla_z T \end{aligned} \tag{12}$$

$$\begin{aligned} j_c &= \left(\sigma_s(E)\sin\theta_h\cos\theta_h\right)\nabla_z\left(\frac{\mu}{e} - \phi\right) - \sigma_s(E)\frac{k}{e}\sin\theta_h\cos\theta_h \\ &\quad \cdot\left(\frac{\varepsilon_o-\mu}{kT} - \Delta_s^*\frac{I_0(\Delta_s^*)}{I_1(\Delta_s^*)} + 2 - \Delta_z^*\frac{I_1(\Delta_z^*)}{I_0(\Delta_z^*)}\right)\nabla_z T, \end{aligned} \tag{13}$$

From Eqs.(12) and (13) the electrical conductivities are given as

$$\sigma_{zz} = \sigma_z(E) + \sigma_s(E)\sin^2\theta_h \tag{14}$$

$$\sigma_{cz} = \sigma_s(E)\sin\theta_h\cos\theta_h \tag{15}$$

where

$$\begin{aligned}
\sigma_z(E) &= \frac{\mathrm{n}_o e^2 \Delta_z d_z^2 \tau I_1(\Delta_z^*)}{\hbar^2\left(1+(\Omega_z\tau)^2\right) I_0(\Delta_z^*)};\\
\sigma_s(E) &= \frac{\mathrm{n}_o e^2 \Delta_s d_s^2 \tau I_1(\Delta_s^*)}{\hbar^2\left(1+(\Omega_s\tau)^2\right) I_0(\Delta_s^*)};\\
\Omega_z &= \frac{eE_z d_z}{\hbar};\\
\Omega_s &= \frac{eE_s d_s}{\hbar};\\
\Delta_i^* &= \frac{\Delta_i}{kT},\ \ i = z,\ s.
\end{aligned}$$

The differential thermoelectric power α is defined as the ratio $\frac{|\nabla(\frac{\mu}{e}-\phi)|}{|\nabla T|}$ in an open circuit. Hence, interesting to us, α along the axial and circumferential directions are obtained from Eq.(12) and Eq.(13) as

$$\begin{aligned}
\alpha_{zz} = &\left[\frac{\sigma_z(E)}{\sigma_z(E)+\sigma_s(E)\sin^2\theta_h}\frac{k}{e}\left\{\frac{\varepsilon_o-\mu}{kT} - \Delta_z^*\frac{I_0(\Delta_z^*)}{I_1(\Delta_z^*)} + 2 - \Delta_s^*\frac{I_1(\Delta_s^*)}{I_0(\Delta_s^*)}\right\}\right.\\
&\left.+\frac{\sigma_s(E)\sin^2\theta_h}{\sigma_z(E)+\sigma_s(E)\sin^2\theta_h}\frac{k}{e}\left\{\frac{\varepsilon_o-\mu}{kT} - \Delta_s^*\frac{I_0(\Delta_s^*)}{I_1(\Delta_s^*)} + 2 - \Delta_z^*\frac{I_1(\Delta_z^*)}{I_0(\Delta_z^*)}\right\}\right]
\end{aligned} \tag{16}$$

$$\alpha_{cz} = \frac{k}{e}\left[\frac{\varepsilon_o-\mu}{kT} - \Delta_s^*\frac{I_0(\Delta_s^*)}{I_1(\Delta_s^*)} + 2 - \Delta_z^*\frac{I_1(\Delta_z^*)}{I_0(\Delta_z^*)}\right] \tag{17}$$

3 Results, Discussion and Conclusion

In this paper, we analysed the differential thermopower of a chiral CNT using the tractable analytical approach developed in [20]. Unlike [20], we included the spatial derivative into the Boltzmann's equation and solved for the distribution function. We calculated the total current in the presence of both electric field and the temperature gradient. We obtained the electrical conductivity σ and the thermopower α. Our expression for σ coincides with that obtained by [20].

The thermopower α is highly anisotropic, depending on the GCA θ_h, the electric field E, temperature T and the real overlapping integrals for jumps along the respective coordinates Δ_z and Δ_s.

For a further understanding of the results, we analysed it numerically. Numerical results for the thermopower dependence of temperature are shown in figure (1a) for fixed values of Δ_z and

differing values of Δ_s (measured in eV). Δ_s varies from $0.015eV$ to $0.31eV$. It is noted that when Δ_s is slightly greater than or equal to Δ_z, i.e. $\Delta_s = 0.015eV, 0.018eV, 0.02eV$, the thermopower α decreases rapidly with increase in temperature T, and at high temperatures it slowly tends to a lower constant value of α, i.e., hyperbolic in nature. This is as expected for semiconducting tubes which exhibit the behaviour $\alpha \sim \frac{1}{T}$ [25]. Meanwhile, when Δ_s is greater than Δ_z, i.e. when $\Delta_s = 0.031eV$, the thermopower increases rapidly, gets to a turning point, then decreases slowly to a constant value. The turning point occurs around $100K$. A similar observation has been noted in [26] where the thermopower of a single-walled carbon nanotube has been measured. It becomes obvious that the material, under these conditions, is behaving as a semi-metal. The thermopower data in Figure (1a) are positive over the entire range of temperature, indicating that the contribution from positive (hole) carriers dominates the response.

As Δ_z increases from $0.015eV$ to $0.024eV$, $0.027eV$, and $0.041eV$ respectively, as can be seen in figures (1b), (1c), and (1d), we observed that most curves were indicating turning points at different temperatures, and eventually at $\Delta_z = 0.027eV$, all the curves have turning points. Comparing our results with the experimentally measured α in [27], we noted that the theoretical curves agree reasonably well with experiment. We believe that a more sophisticated energy spectrum will be required but in that case, we shall lose the analytical tractability of the problem. What is striking is that the turning points occur in two situations, i.e., when Δ_z is quite greater than Δ_s and vice versa. The turning points shift towards lower temperatures for given Δ_z, but they shift towards greater temperatures as Δ_z increases. One also notes that there exists a threshold temperature for which hole conductivity switches over to electron conductivity, i.e., positive α becomes negative. This can be explained by the fact that graphite has a pair of weakly overlapping electron and hole sp^2 or π band with near mirror symmetry about the Fermi energy E_F. Approximately, equal numbers of electrons and holes in these symmetric π bands are consistent with the negative thermopower observed [27]. The threshold value for the temperature shifts towards lower temperature as we increase Δ_z.

In figures (2a) and (2b), it became clear that for greater values of Δ_z, thermopower α becomes completely n-type and hyperbolic, i.e. $\alpha \sim \frac{1}{T}$ [25]. We observed in figure (2b) that at about $600K$ onwards, α becomes $0\frac{V}{K}$. A similar observation was made for armchair symmetry tubes [26]. This was attributed to the mirror symmetry of the coexisting electrons and holes in the overlapping π bonds. Kong *et al.* [28], in their recent report on SWNT chemical sensors, refer to extrinsic p-type behaviour in their isolated semiconducting SWNT, whilst previously published large positive thermopower data was attributed to intrinsic SWNT behaviour [29].

Finally, we summarised our results with 3 dimensional sketches in figure (3a) and (3b) It is worthy to note that when $d_s = d_z$ and $\Delta_s = \Delta_z$ as stated in [20], we have a transition from a chiral nanotube to a (monolayer) planer graphite sheet as expressed in the isotropic conductivity σ and thermopower α.

It is known that the choice of materials for thermodevices, be it generators, thermocouples

or refrigerators, is based on thermoelectric figure of merit Z defined by the relation

$$Z = \frac{\alpha^2 \sigma}{\chi}$$

where χ is the thermal conductivity. In our opinion the electrical power factor $\alpha^2\sigma$ involved in Z can be enhanced drastically in CNT by optimizing the choice of the T, Δ_s, Δ_z and θ_h as indicated in the results.

In conclusion, the differential thermopower of chiral CNT has been investigated theoretically. An excellent analytical expression has been found for σ and α. The determination of α can be used to determine whether the CNT is semimetal or semiconductor. Again, the cost in production of CNT, we hope, is cheaper and less sophisticated than superlattice, and hence, can be good material for a thermoelement.

Acknowledgements

This work was done within the framework of the Associateship Scheme of the Abdus Salam International Centre for Theoretical Physics, Trieste Italy. Financial support from the Swedish International Development Cooperation Agency is acknowledged. We also want to acknowledge C. K. W. Adu for useful discussions.

References

[1] T. Ebbeson, *Phys. Today* **49** 6 26 (1996).

[2] S. Ijima, *Nature (London)* **54** 56 (1991).

[3] N. M. Rodriguez, *J. Mater. Res.* **8** 3233 (1993).

[4] J. W. Mintmire, B. I. Dunlap and C. T. White, *Phys. Rev. Lett.* **68** 631 (1992).

[5] R. Saito, M. Fujita, G. Dresselhaus and M. S. Dresselhaus, *Appl. Phys. Lett.* **60** 2204 (1992).

[6] N. Hamada, S. Sawada and A. Oshiyama, *Phys. Rev. Lett.* **68** 1579 (1992).

[7] J. W. Mintmire, D. H. Robertson and C. T. White, *J. Chem. Phys. Sol.* **54** 1835 (1993).

[8] C. Kane, L. Balents and M. P. A. Fisher, *Phys. Rev. Lett.* **79** 25 5086 (1997).

[9] J. M. Bonard, J. P. Salvetat, T. Stockli and W. A. de Heer, *Appl. Phys. Lett.* **73** 918 (1998).

[10] Q. H. Wang, T. D. Corrigan, T. Y. Dai and R. P. H. Chang, *Appl. Phys. Lett.* **70** 3308 (1997).

[11] W. A. de Heer, A. Chatelain and D. Ugarte, *Science*, **270** 1179 (1995).

[12] S. Han and J. Ihm, *Phys. Rev. B* **61** 15 9986 (2000).

[13] P. Kim, T. W. Odom, J. L. Huang and C. M. Lieber, *Phys. Rev. Lett.* **82** 6 1225 (1999).

[14] O. V. Kibis, *Fiz. Tverd. Tela,* **34** 3511 (1992) [*Sov. Phys. Solid State* **34** 1880 (1992)].

[15] D. A. Romanov, *Pis'ma Zh. Eksp. Teor. Fiz,* **55** 703 (1992) [*JETP Lett.* **55** 738 (1992)].

[16] O. V. Kibis and D. A. Romanov, *Fiz. Tverd. Tela,* **37** 127 (1995) [*Phys. Solid State,* **37** 69 (1995)].

[17] L. Chico, V. H. Crespi, L. X. Benedict, S. G. Louie and M. L. Cohen, *Phys. Rev. Lett.* **76** 971 (1996).

[18] L. Langer, V. Bayot, E. Grivei, J. P. Issi, J. P. Heremans, C. H. Oik, L. Stockman, C. Van Haesendonck and Y. Bruynseraede, *Phys. Rev. Lett.* **76** 479 (1996).

[19] L. M. Woods and G. D. Mahan, *Phys. Rev. B* **61** 16 10651 (2000).

[20] G. Ya. Slepyan, S. A. Maksimenko, A. Lakhtakia, O. M. Yevtushenko, and A. V. Gusakov, *Phys. Rev. B* **57** 16 9485 (1998).

[21] Y. Miyamoto, S. G. Louie and M. L. Cohen, *Phys. Rev. Lett.* **76** 2121 (1996).

[22] A. Yu. Kasumov, I. I. Khodos, P. M. Ajayan and C. Colliex, *Europhys. Lett.* **34**, 429 (1996).

[23] R. D. Rowe, G. Hin and V. L. Kuznestsov, *Phil. Mag.* **77** 2 105 (1998).

[24] S. Y. Mensah and G. K. Kangah, *J. Phys.: Condens. Matter,* **4** 919 (1992).

[25] G. U. Sumanasekera, C. K. W. Adu, S. Fang and P. C. Eklund, *Phys. Rev. Lett.* **85** 5 1096 (2000).

[26] J. Hone, I. Ellwood, M. Muno, Ari Mizel, Marvin L. Cohen and A. Zettl, *Phys. Rev. Lett.* **80** 1042 (1998).

[27] L. Grigorian, G. U. Sumanasekera, A. L. Loper, S. L. Fang, J. L. Allen and P. C. Eklund, *Phys. Rev. B* **60** R11 309 (1999).

[28] Kong et al., *Science*, **287** 622 (2000).

[29] L. Grigorian et al., *Phys. Rev. Lett.* **80** 5560 (1998).

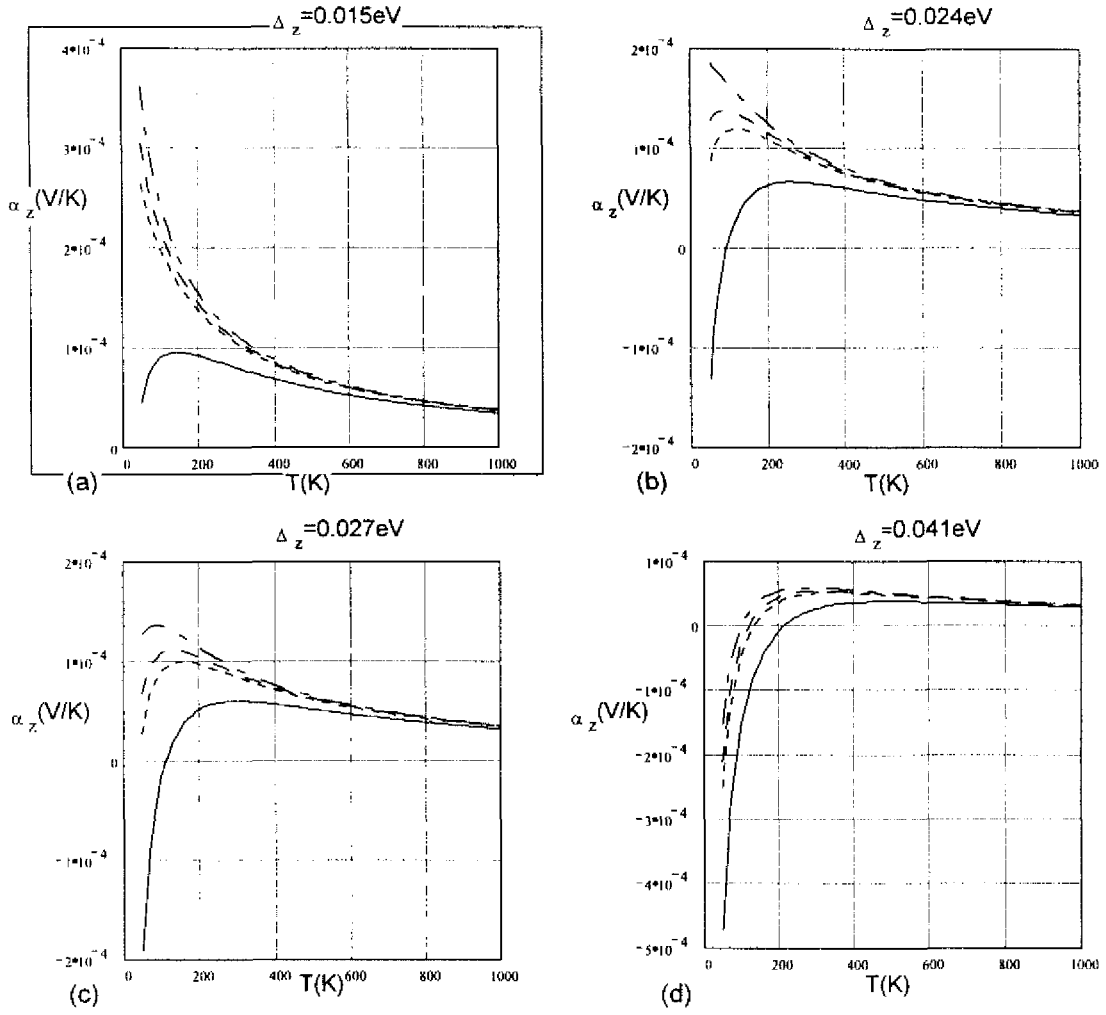

Figure 1: *The dependence of thermopower α on temperature T for Δ_s equal to* $0.015eV$ (— - —), $0.018eV$ (— —), $0.020eV$ (- - -) *and* $0.031eV$ (——) *for differing values of* Δ_z*: (a)* $\Delta_z = 0.015eV$*, (b)* $\Delta_z = 0.024eV$*, (c)* $\Delta_z = 0.027eV$*, and (d)* $\Delta_z = 0.041eV$.

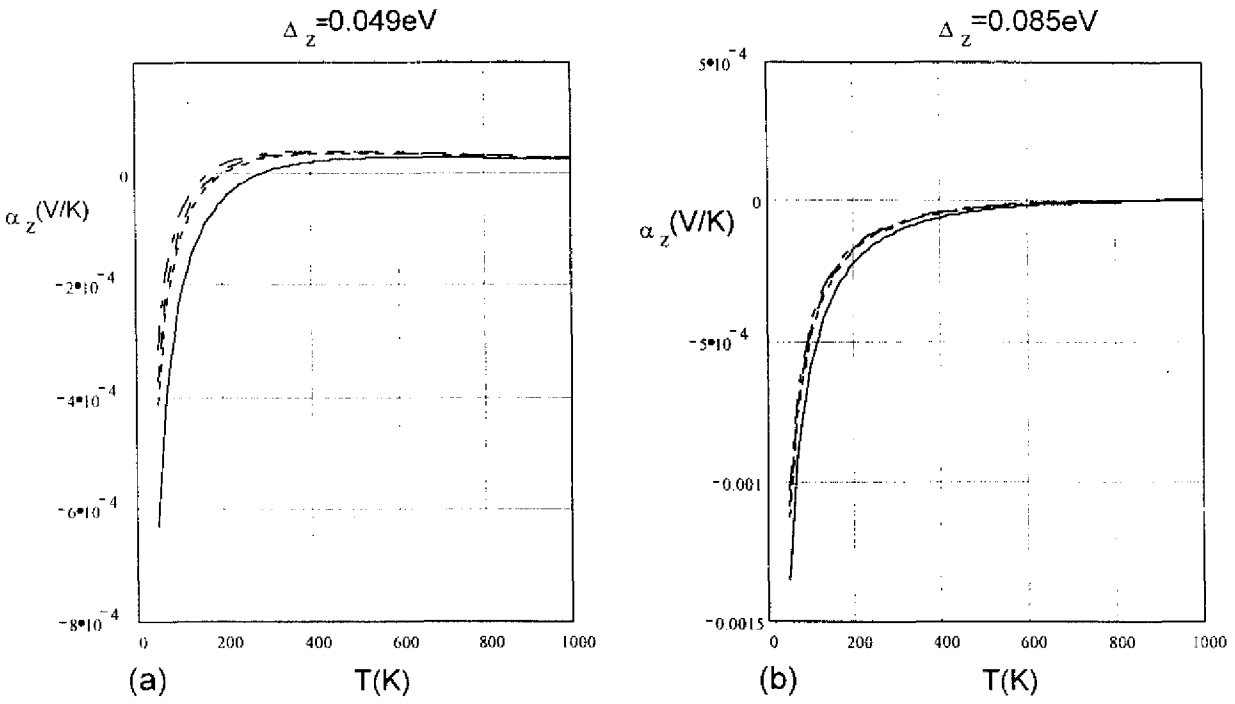

Figure 2: *The dependence of thermopower α on temperature T for Δ_s equal to* $0.015eV$ (— - —), $0.018eV$ (— —), $0.020eV$ (- - -) *and* $0.031eV$ (——) *for (a)* $\Delta_z = 0.049eV$*; (b)* $\Delta_z = 0.085eV$.

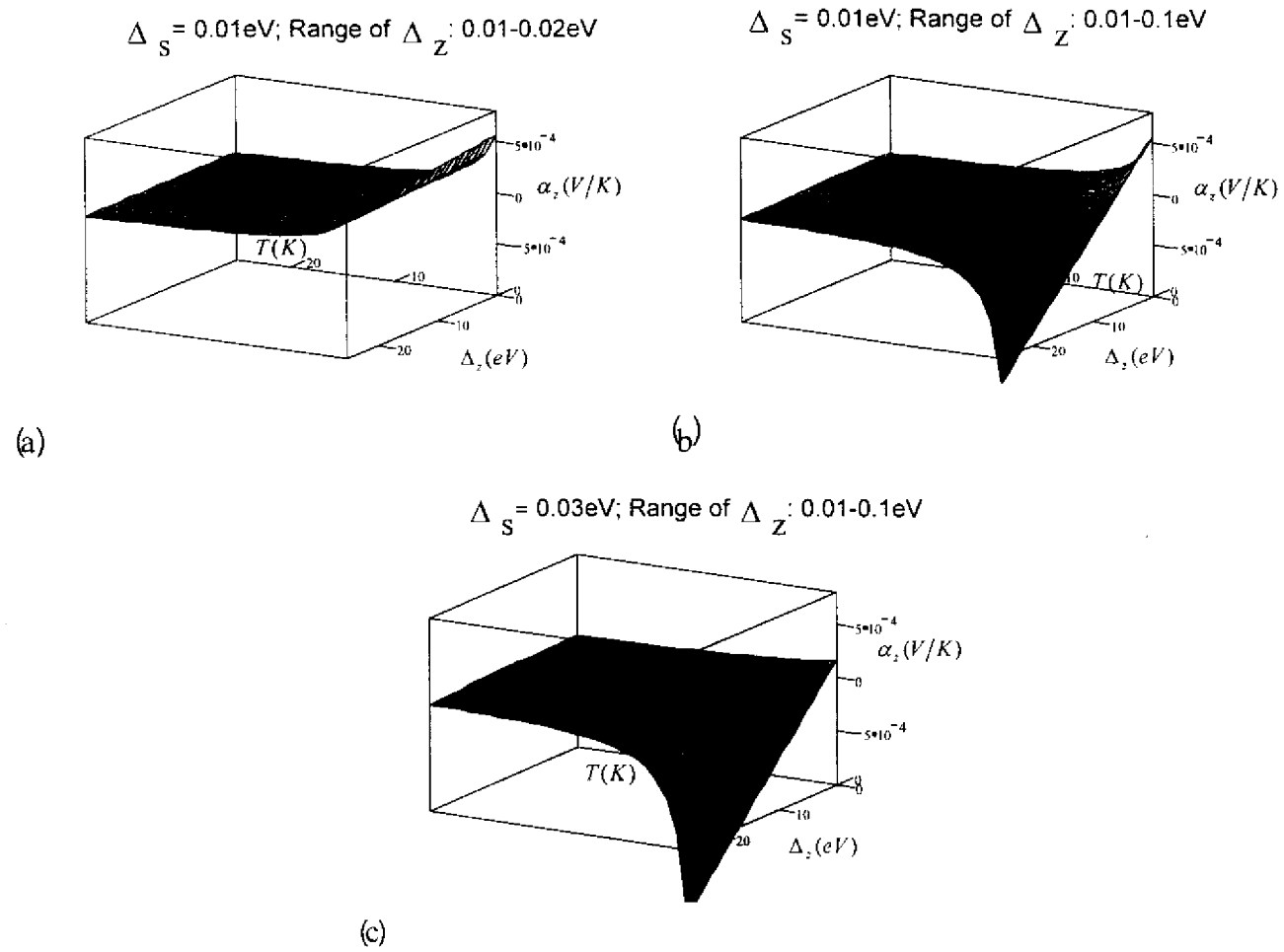

Figure 3: *3-dimensional sketches of* $\alpha_z(T, \Delta_z)$*: (a)* $\Delta_s = 0.01eV$ *and* $0.01eV \leq \Delta_z \leq 0.02eV$*; (b)* $\Delta_s = 0.01eV$ *and* $0.01eV \leq \Delta_z \leq 0.1eV$*; (c)* $\Delta_s = 0.03eV$ *and* $0.01eV \leq \Delta_z \leq 0.1eV$ *. In (a), 1 unit :* $4.0 \times 10^{-4}eV$ *on* Δ_z *axis; and 1 unit :* $38K$ *on* T *axis. In (b), (c) and (d), 1 unit :* $3.6 \times 10^{-2}eV$ *on* Δ_z *axis; and 1 unit :* $38K$ *on* T *axis.*